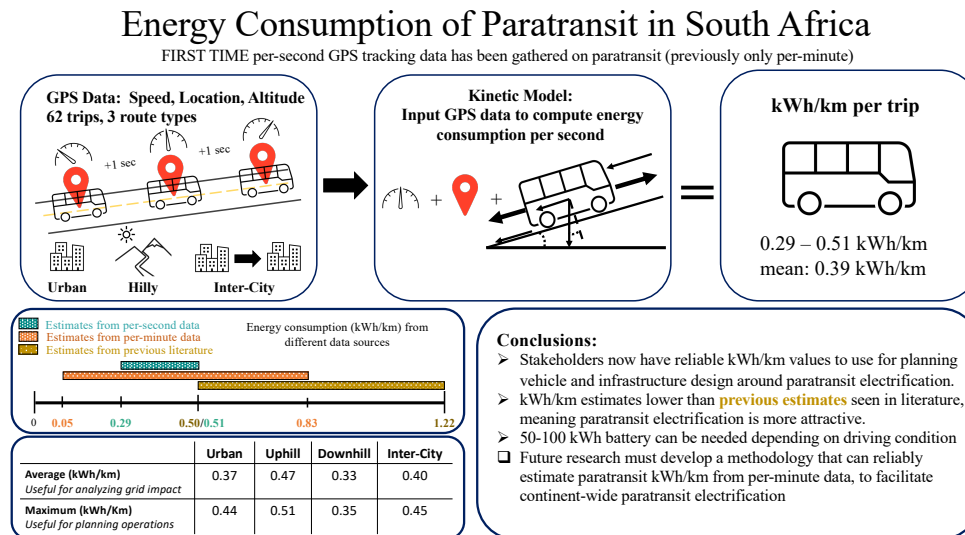


Using high resolution GPS data to plan the electrification of paratransit: A case study in South Africa

Highlights

- Highest fidelity energy consumption estimates (kWh/km) for paratransit to date.
- Urban, hilly, and inter-city driving conditions are investigated.
- Estimates from 0.29 – 0.51 kWh/km (mean = 0.39 kWh/km), depending on driving condition
- Specific kWh/km recommendations given for usage in operations planning and grid impact.
- Per-minute data fails to capture the effect of micro-mobility patterns on energy consumption.

Graphical abstract



Using high resolution GPS data to plan the electrification of paratransit: A case study in South Africa

Christopher Hull ^{a,*}, J.H. Giliomee ^b, Katherine A. Collett ^a, Malcolm D. McCulloch ^a, M.J. Booysen ^{b,**}

^a*Energy and Power Group at the Engineering Science Department, University of Oxford, United Kingdom*

^b*Department of E&E Engineering, Stellenbosch University, South Africa*

Abstract

Paratransit is the mainstay of public transport in sub-Saharan Africa, and minibuses are the most common form of paratransit. These minibuses are often second-hand, ageing, fuel inefficient, and expensive to operate - issues that electrification can help solve. However, modeling and planning large-scale transitions to electric paratransit require reliable estimates of vehicle energy consumption. This paper provides high fidelity energy consumption estimates by applying a vehicle kinetic model to per-second GPS data gathered on minibus taxis. The data include 62 trips across three routes with different driving conditions in South Africa. The conditions were urban, hilly, and inter-city. We find a range of energy consumption from 0.29 to 0.51 kWh/km (mean = 0.39 kWh/km). We recommend kWh/km rates for modeling operations and grid impact in each condition, and discuss how future work can utilize our analysis to advance the electrification transition in sub-Saharan Africa. We quantify the effects of elevation change, speed, and acceleration on energy consumption. Past literature estimating paratransit energy consumption has relied on per-minute GPS data. A comparison of model results with per-minute and per-second data, and Fast Fourier Transformations, shows that per-minute data fails to capture micro-mobility patterns, leading to inaccurate energy consumption estimates.

Keywords: Electric Vehicles, Energy Transition, Energy Consumption, Energy Planning, Infrastructure Planning, Transportation

1. Introduction

This paper aims to provide high fidelity energy consumption estimates (kWh/km) for electric paratransit vehicles in South Africa. Establishing per-distance energy consumption for electric vehicles (EV) is necessary for planning operations, sizing vehicle batteries, determining appropriate charging infrastructure, and managing vehicle impact on the grid. The availability of high fidelity energy consumption estimates is paramount for the optimization of these models, and thus critical for stakeholders in governments, charge point manufacturers and operators, fleet managers, vehicle manufacturers, utilities companies, network operators, and city planners to effectively plan large-scale transitions to EVs. We provide specific recommendations for kWh/km values to use for these models.

Transport accounts for roughly third of global energy consumption, and is responsible for about 16% of global emissions, and the development of low-carbon transport in cities is part of the global agenda to mitigate climate change and relates to at least three of the United Nation's Sustainable Development Goals [1]. Accordingly, EV sales have seen substantial growth in the Global North and many global vehicle manufacturers and governments seek to stop production of combustion engines altogether as early as 2035 [2, 3, 4]. In contrast, due to low electricity access and high upfront costs [5], the transition to more expensive EVs has been painstakingly slow in sub-Saharan Africa (SSA). Africa is a major destination for old and used vehicles, which typically consume particularly dirty fuel such as diesel with high-sulfur content. This not only causes serious air pollution and health problems in African cities, but contributes heavily to greenhouse

*Corresponding author

**Corresponding author

Email addresses: christopher.hull@eng.ox.ac.uk (Christopher Hull), mjbooyesen@sun.ac.za (M.J. Booysen)

gas emissions [6]. The fuel for these vehicles is typically imported, leaving these countries with issues related to fuel quality, energy security and price fluctuations [6].

Privately-owned minibus taxis are ubiquitous in the developing cities and rural areas of SSA. They form a substantial part of the "paratransit" system – an informal transport sector common in the region. Paratransit travel comprises at least 90% of road-based public trips in Lagos, Kampala and Dar es Salaam [7, 8], of which 83% are by minibus taxi [9, 8, 10]. In South Africa, minibus taxis form the entire paratransit industry, which is worth \$3.7bn. Every day, over 300,000 minibus taxis carry out approximately 15 million trips, amounting to more than 73% of daily commuters [11]. In the face of the increasing demand for urban commuting heralded by urbanization and population growth, electrifying minibus taxis becomes even more critical for meaningful transport sector decarbonization in sub-Saharan Africa (SSA) [12, 13].

This informal sector is now faced with the need to transform to an electrical energy source [8, 9, 7, 14]. However, electricity grids in the region are energy-constrained, which affects the feasibility of converting to EVs. In addition, many stakeholders and decision makers are capital constrained, and thus investment must be carefully considered. Therefore, before commencing a large scale transition, it is crucial to establish high fidelity estimates of minibus taxi energy requirements, based on their micro-mobility patterns across driving conditions. Without high fidelity estimates, it would be difficult for stakeholders to plan operations, size viable vehicle batteries, manage EV impact on the grid, and design appropriate charging infrastructure.

The driving cycles and the concomitant energy requirements of electric passenger vehicles and larger buses in higher-income countries are well established and deeply analyzed [15, 16, 17, 18, 19], and there are energy consumption estimates for minibuses in developed contexts [20]. Nevertheless, there is a distinct lack of high fidelity analysis for paratransit in SSA. Given the unique mobility patterns and unconventional driving styles of African paratransit, high-income country conventional driving cycles do not apply to these contexts [21].

To estimate vehicle energy consumption, we apply a vehicle kinetic model to per-second GPS data gathered on trips taken on internal combustion engine (ICE) minibus taxis to model how much energy would be required to power an electric equivalent. To date, estimations of energy consumption for electric paratransit in SSA have been either based on data captured at a sampling frequency of once per minute [22, 23], or have been forced to a conservative simplifying assumption due to a lack of data [24]. However, paratransit vehicle drivers have been reported to engage in aggressive maneuvers characterized by sharp acceleration and/or deceleration movements that last mere seconds, and for making numerous quick stops to continuously pick up and drop off passengers [25]. The energy intensity of aggressive micro-mobility patterns have been observed to have a great effect on per-distance energy consumption [26, 27, 28, 29]. Therefore, following the Nyquist-Shannon sampling theorem [30], we hypothesize that a sampling frequency that provides several samples per movement is needed to capture their effect on energy consumption. This paper aims to fill this gap in the literature and improve stakeholder confidence in paratransit vehicle energy consumption estimates by utilizing per-second GPS data that can capture vehicle micro-mobility patterns to provide high fidelity energy consumption estimates. After presenting our main results, we verify that per-second data provides higher fidelity estimates than per-minute data.

Another overlooked aspect in the literature is disaggregating energy consumption estimates by driving conditions. EV energy consumption is known to be highly dependent on driving conditions with different elevation, speed, and micro-mobility patterns [26, 31, 32], and previous literature has not provided kWh/km estimates for different driving conditions. To fill this gap in the literature and capture the effect of variation in driving conditions on energy consumption, this paper uses data captured on urban, hilly, and inter-city routes. We hypothesized that time of day may also have an effect on traffic patterns, so for each route we captured data in the morning, afternoon, and evening.

Our high fidelity estimates can be used to establish a benchmark for paratransit energy consumption. Once established, such a standard could be used to validate future energy consumption estimates from per-minute data in various locations and driving conditions. This is useful since gathering high-resolution data for vehicles across many different contexts would be time and labor intensive. There are mobility companies such as WhereIsMyTransport and GoMetro that already capture telemetry data for minibus taxis at a resolution of once per-minute in many cities around SSA to create spatial mobility models for operations and route planning, and there is potential for substantial benefit to being able to take advantage of this data that already exists or is being gathered. Thus, while providing high fidelity vehicle energy consumption estimations for minibus taxis in South Africa that can be used immediately, this paper provides a platform for future research to develop accurate methods of estimation based on per-minute data input. For example, developing a micro-

traffic simulator, based on the micro-traffic mobility patterns we see in the per-second data, which can intake per-minute data and accurately model taxi driver behavior in between waypoints. With such a tool, per-minute travel data could be fed into a micro-traffic simulator to come up with reliable energy consumption estimations for paratransit in many different locations. Figure 1 shows how this validation process can feed into large-scale EV and infrastructure design.

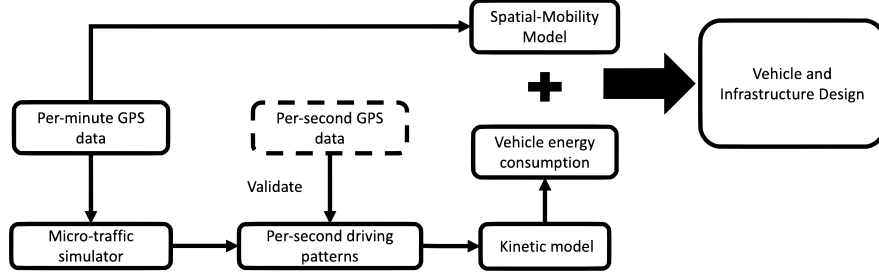


Figure 1: How per-second GPS data can support EV and infrastructure design by validating energy consumption estimates derived from GPS per-minute data.

2. Methodology

To construct high fidelity energy consumption estimates for minibus taxis: i) a kinetic model is required to establish energy demand from motion based on GPS data, and ii) granular GPS data from representative journeys is necessary. Figure 2 visualizes at a high level the process for using GPS data and a kinetic model to construct energy consumption estimates.

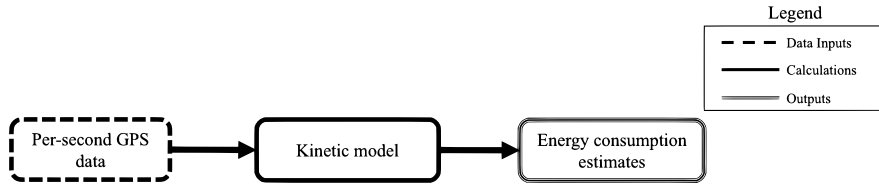


Figure 2: How per-second GPS data is used to estimate energy consumption via a kinetic model

2.1. Kinetic model

The objective of the kinetic model is to estimate the energy consumed by the vehicle over the duration of a trip. In this section, we provide background on kinetic models seen in the literature, justify the principles behind the construction of our kinetic model, and describe our model mathematically.

All vehicle kinetic models are derived from the same fundamental principles of physics, which inform us that the instantaneous power output of an EV is a function of its velocity, acceleration, and the slope angle it faces. However, kinetic models in the literature often differ slightly; various kinetic models have been employed to provide estimations of EV energy consumption based on GPS travel data [33, 34, 35, 36, 37]. The fundamental laws of physics cannot change, so these variations come from discrepancies based on assumptions from empirical data or fitted model parameters. Validation with ground-truth data has shown that these variations can have an effect on model performance [38].

For example, Sagaama et al. [38] show that the accuracy of the kinetic model integrated in the micro-traffic simulator SUMO (Simulation Of Urban MObility) improves when applying a certain dynamic regenerative braking formula in favor of a static regenerative braking factor. We find that adding this dynamic regenerative braking formula into our kinetic mode decreases mean vehicle energy consumption across all trips by 15% (from 0.39 kWh/km to 0.33 kWh/km), a substantial margin. A key assumption in this dynamic formula is that the drivers are making full use of regenerative braking every time they decelerate. However, in this context, given the taxi drivers' lurching driving style and heavy usage of brake pads, this means the dynamic formula will overestimate the energy recuperated back into the battery. For this reason, our kinetic model does not use a dynamic regenerative braking formula. Instead, we apply a static regenerative braking factor that is not subject to being highly influenced by extreme deceleration events.

Sagaama et al. [38] also show that ambient air temperature can have an effect on power offtake. A limitation of our dataset is that temperature data was not available. However, given that a) the dynamic power offtake evaluated in Sagaama et al. [38] was not constructed for paratransit contexts and b) there is a paucity of low-voltage auxiliary power applications on board paratransit, it is not likely in the authors' estimation that this would have a) increased model accuracy or b) significantly affected the results.

While some empirical assumptions and fitted model parameters have been validated in developed contexts with ground-truth benchmark of real per-second EV energy consumption data [34, 35], these results do not necessarily extrapolate to sub-Saharan African paratransit driving contexts. Furthermore, the motivation of this paper is to provide high fidelity vehicle energy consumption estimations, not a novel kinetic model. Therefore, to avoid concern that our energy consumption estimates are potentially skewed by underlying empirical assumptions or fitted model parameters, the model we employ is based solely on fundamental principles of physics.

While we entirely avoid basing our kinetic model on empirical assumptions or fitted model parameters, any kinetic model must employ some specific vehicle constant parameters to obtain EV energy consumption estimates. These constant parameters along with the relevant references are listed in Table 1.

To compute energy consumption over the duration of a trip, we use per-second GPS data to separately compute either the energy out of the battery to turn the wheels or power auxiliary functions, or the energy flow into the battery from regenerative braking at each sample's time step n , $E[n]$. We then sum the estimate at each time step to obtain entire trip's energy consumption $E_{\text{trip}} = \sum E[n]$.

To determine energy flow at each time step, $E[n]$ in (kWh), we implement the following five-step algorithm:

- 1) Compute the sum of all external forces on the vehicle for sample n at a sample period of τ , $F_{\text{ext}}[n]$ in (N), using

$$F_{\text{ext}}[n] = -F_{\text{ad}}[n] - F_{\text{rs}}[n] - F_{\text{rr}}[n] \quad (1a)$$

Where $F_{\text{ad}}[n]$ is the aerodynamic drag, $F_{\text{rr}}[n]$ is the rolling resistance friction, and $F_{\text{rs}}[n]$ is the slope drag force (positive for incline or negative for decline). The forces are shown in Figure 3.

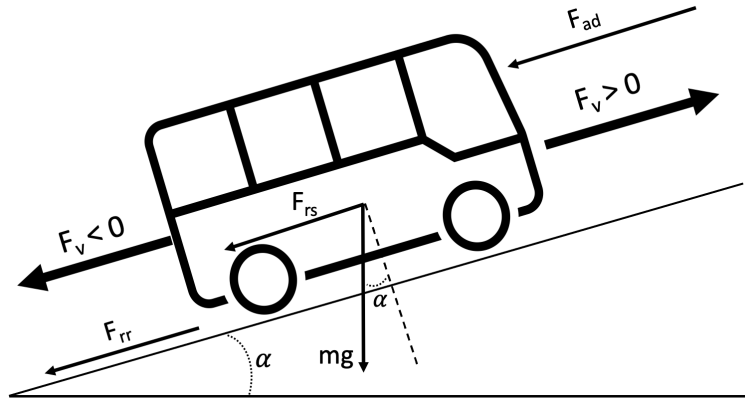


Figure 3: The forces acting on a vehicle driving on a slope: Aerodynamic drag (F_{ad}), rolling resistance (F_{rr}), slope drag (F_{rs}), and vehicle force (F_v) which can be either positive or negative depending on whether the vehicle is accelerating or decelerating. F_v is shown with thicker lines as it is usually the greatest force, since it must overcome other forces in order to accelerate or decelerate the vehicle.

Parameter	Symbol	Value	Ref.
Gravitational acceleration	g	9.81 m/s ²	–
Density of air at 25°C	ρ	1.184 kg/m ³	[39]
Power offtake	p_0	100 W	[40]
Minibus weight	m_v	3900 kg	[41]
Drag coefficient	c_d	0.36	[42]
Rolling resistance coefficient	c_{rr}	0.02	[39]
Vehicle's front surface area	A	4 m ²	[43]
Powertrain efficiency	μ_v	90%	[44]
Regenerative braking efficiency	μ_{rg}	65%	[45]

Table 1: Constants and parameters used in kinetic model.

The forces in Figure 3 are individually calculated from fundamental physics using the following equations and the constants listed in Table 1.

$$F_{ad}[n] = \frac{1}{2} \rho c_d A (v[n])^2 \quad (1b)$$

$$F_{rr}[n] = \begin{cases} m_v g c_{rr} \cos(\alpha[n]), & \text{if } v[n] > 0.3 \text{ m/s (GPS noise threshold)} \\ 0, & \text{otherwise} \end{cases} \quad (1c)$$

$$F_{sd} = m_v g \sin(\alpha_t) \quad (1d)$$

where

$$\alpha[n] = \begin{cases} \arcsin\left(\frac{h[n]-h[n-1]}{s[n]}\right) & \text{if } |h[n] - h[n-1]| > 0.1 \text{ m (GPS noise threshold)} \\ 0, & \text{otherwise} \end{cases}$$

2) Compute the expected change in velocity (in m/s) if $F_{ext}[n]$ were the only force applied to the vehicle.

$$dv_{exp}[n] = \frac{F_{ext}[n]}{m_v} \tau \quad (2)$$

3) Any difference between the expected velocity and measured velocity, v_{meas} , is ascribed to the acceleration or deceleration force applied by the vehicle, F_v , calculated by:

$$F_v[n] = \frac{v_{meas}[n] - v_{exp}[n]}{\tau} m_v \quad (3)$$

4) When $F_v[n] > 0$, energy in (Ws) was **discharged from** the battery to apply propulsion to the vehicle.

$$E_{prop}[n] = \frac{F_v[n] v[n] \tau}{\mu} \quad (4a)$$

When $F_v[n] < 0$, energy in (Ws) was **charged into** the battery via regenerative braking:

$$E_{regen}[n] = \mu_{rg} F_v[n] v[n] \tau \quad (4b)$$

The energy discharge from the battery simply to keep the vehicle running is defined as power offtake. For every measured time interval, power offtake in (Ws) is calculated by

$$E_{offtake}[n] = p_0 \tau. \quad (4c)$$

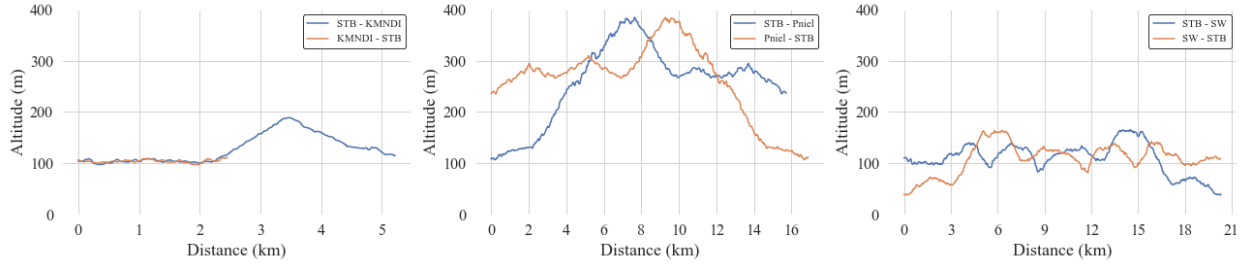
5) Compute the total energy flow in a given time-step $E[n]$ in (kWh) by summing the propulsive, regenerative, and constant off-take energies.

$$E[n] = \frac{E_{prop}[n] + E_{regen}[n] + E_{offtake}[n]}{3.6 \times 10^6} \quad (5)$$

Finally, we can compute the energy consumption over the whole trip in (kWh) by summing over the



(a) Bird's eye view of the three routes selected for data capture [47].



(b) Altitude plots for the three routes. Outbound trips are shown in orange, and inbound trips are shown in blue. The trip from Stellenbosch to Kayamandi includes an extra circular segment inside the township, making the trip roughly twice as long as its counterpart.

Figure 4: The routes used to assess vehicle energy consumption in and around Stellenbosch and their altitude profiles.

duration of the trip N .

$$E_{\text{trip}} = \sum_{n=0}^N E[n] \quad (6)$$

2.2. GPS Data Collection

To determine the micro-mobility behavior of the minibus taxis, six tracking devices were used to record GPS data to an SD card at a frequency of 1 Hz.

The velocity, $v[n]$, was obtained from the GPS sample's speed value. The elevation, $h[n]$, was obtained from the GPS sample's location value, which was used to lookup the elevation in the Earth Resources Observation and Science Center's dataset [46]. This method was preferred because the GPS module's elevation values proved to be less consistent than using the location-based lookup. The displacement, $s[n]$, is calculated as the 3D geodesic distance from subsequent GPS locations. The slope angle (positive for incline and negative for decline), $\alpha[n]$, is calculated from subsequent displacements, $s[n-1]$ and $s[n]$, and corresponding elevations, $h[n-1]$ and $h[n]$.

2.3. Route selection

Vehicle energy consumption was expected to be dependent on driving conditions, specifically changes in elevation with or against gravity, driving speed in inter-city transport, and the stop-start nature of urban driving [26]. Time of travel during the day was also expected to have an impact. Therefore, data was captured on three different types of route: urban, hilly, and inter-city. Data for each route was collected at three distinct times of the day: morning (before 11:30AM), afternoon (11:30AM - 4:30PM), and evening (after

4:30PM). All trips are recorded from, or back to, Bergzicht Taxi Rank, the main taxi rank in Stellenbosch, South Africa, and are shown in Figure 4.

The urban route is from Stellenbosch to Kayamandi taxi rank (STB - KMNDI). Kayamandi is a neighborhood of Stellenbosch with a proportion of taxi riders. The routes connecting the taxi ranks have a speed limit of 60 km/h and consist of bidirectional roads only. The to and from routes vary slightly, since the taxis pass the Kayamandi taxi rank and completes a circle route through the neighborhood, dropping off passengers near their homes, before returning to the Kayamandi rank for the routine stop. The distances to and from Kayamandi taxi rank are 5 km and 2.6 km respectively.

The hilly route is one with a steep incline from Stellenbosch to Pniel (STB - Pniel) and crosses the Helshoogte mountain pass – a steady climb of approximately 300 m in 7 km. This 12.5 km route, with a small deviation on some trips, features a long accent followed by a short decent, and has a speed limit of 80 km/h.

The inter-city route is a 20 km route from Stellenbosch to Somerset West (STB - SW). The speed limit on this provincial road, which is predominantly a dual carriageway, is 100 km/h.

Table 2 shows the breakdown of data collected after filtering for trips with missing or anomalous data. The goal was to collect at least three trips for each route and time of day combination to establish a reasonable depth of data for each driving context. After data cleaning, this was successful for all route/time of day combinations except for Pniel - STB/’Evening’, which was left with 2 trips. The final number of trips used for analysis was 62.

	Route						Total
	Stellenbosch Kayamandi	Kayamandi Stellenbosch	Stellenbosch Pniel	Pniel Stellenbosch	Stellenbosch Somerset West	Somerset West Stellenbosch	
<i>Distance:</i>	5 km	2.6 km	15 km	15 km	20 km	20 km	
<i>Avg. Time:</i>	18 min	6 min	28 min	23 min	29 min	27 min	
<i>Speed Limit</i>	60 km/h	60 km/h	80 km/h	80 km/h	100 km/h	100 km/h	
Morning	4	4	3	3	3	3	20
Afternoon	3	5	4	4	4	4	24
Evening	3	3	3	2	4	3	18
Total	10	12	10	9	11	10	62

Table 2: Summary of the number of trips recorded in data acquisition phase.

A preview of the dataset is publicly available in this repository: <https://doi.org/10.17632/xt69cnwh56.1>. A data-in-brief has been submitted for review.

2.4. Comparing per-second and per-minute GPS data input

To evaluate model performance using per-second versus per-minute data, we must construct an equivalent per-minute dataset. To do so, we first downsample our per-second data to one GPS observation per minute using python pandas resample function. We start from the first sample, and take one sample every minute thereafter. We then feed this per-minute data into our kinetic model to generate energy consumption estimations, and compare that to our original results. This process is shown in Figure 5.

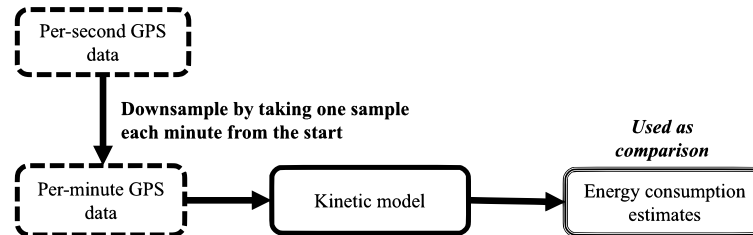


Figure 5: How an equivalent per-minute dataset created from the raw per-second data and used to construct energy consumption results. These results are then compared with the results generated by the process in Figure 2.

3. Results

3.1. Evaluation of energy consumption estimates

In this section, we first present our energy consumption estimates in kWh/km and evaluate the differences seen between the various driving conditions and times of day. We then compare our results to values previously seen in the literature.

3.1.1. Impacts of route and time of day

Figure 6 shows the distributions of energy consumption estimates for the three routes considered, in both directions, for each time of day (yielding a total of $3 \times 2 \times 3 = 18$ distributions). A dashed teal line indicates the overall mean of 0.39 kWh/km. This figure demonstrates how energy consumption is largely determined by the characteristics of the route on which a minibus is driving. The route characteristic with the clearest effect is elevation change, as evidenced by the difference observed between the steep incline and steep decline directions of the hilly route (to/from Pniel). Additionally, it appears that the inter-city travel (to/from SW) was slightly more energy intensive per kilometer on average than urban travel (to/from KMNDI).

Although distinctive patterns are observed between routes, the results do not show a consistent effect of time of day on energy consumption on any route. The estimates are within a fairly tight range for each route, with a mean inter-route standard deviation of 0.02 kWh/km, which supports the hypothesis the per-second sampling strategy leads to high fidelity estimates.

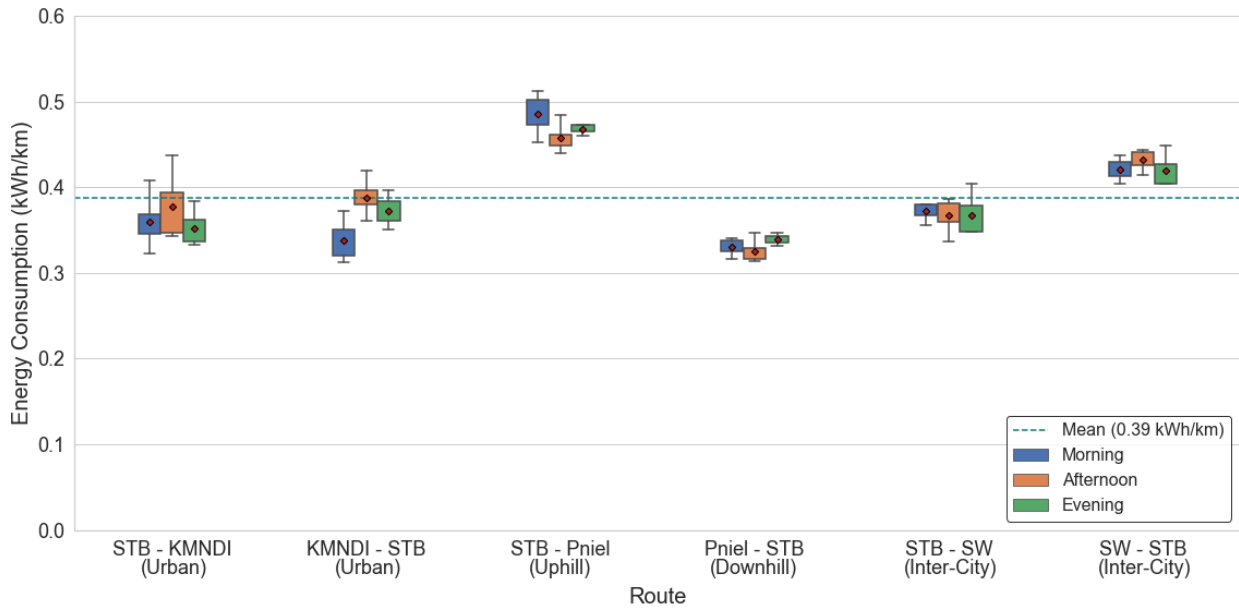


Figure 6: Distribution of energy consumption for each route in the morning, afternoon, and evening. The overall mean energy consumption of 0.39 kWh/km is indicated with a dashed teal line.

Table 3 summarizes the mean energy consumption and some mobility characteristics observed for each of the routes. This table shows the variation in the physical nature of the routes and some factors that characterize traffic flow (i.e. speed and how often the vehicle must stop). The urban route had the highest average absolute acceleration and lowest speeds, belying the stop-start nature of urban travel. The effect of this driving pattern on energy consumption is explored in later sections. The average of absolute acceleration is used to account for total acceleration and deceleration.

3.1.2. Results in context

To contextualize our energy consumption results, we compared them to values seen in the literature and real world manufacturer-stated kWh/km for similar vehicles. Table 4 lists these values and their sources.

Route	Energy Consumption (kWh/km)	Net Elevation Change (m)	Average Speed (km/h)	Maximum Speed (km/h)	Average Acceleration (absolute) (m/s ²)
STB - KMNDI	0.36	12.7	15.9	64.2	0.52
KMNDI - STB	0.37	1.3	26.1	70.7	0.57
STB - SW	0.37	-68.1	42.5	101.4	0.50
SW - STB	0.42	67.5	44.2	98.5	0.49
STB - Pniel	0.47	126.7	33.3	84.0	0.48
Pniel - STB	0.33	-127.2	40.4	90.2	0.52

Table 3: Breakdown of average energy consumption, net elevation change, average speed, maximum speed, and average absolute acceleration by route.

Figure 7 displays our distributions of energy consumption results for each route in comparison to the values in Table 4. Since time of day was found to have no effect on energy consumption in section 3.1.1, we aggregate times of day by route for a more concise comparison.

Our results are slightly higher than the energy consumption of small passenger vans on the market, which range from 0.21 - 0.36 kWh/km. This is logical given that taxi drivers are notorious for aggressive driving, which increases energy consumption [26, 27, 28, 29]. Seeing values that are similar to but slightly higher than manufacturer given values lends confidence to the accuracy of our estimates.

In contrast, our estimates – barring one uphill trip at 0.51 kWh/km – were lower than the comparative values from literature, which ranged from 0.50 to 0.93 kWh/km. Notably, the highest results previously in the literature from Abraham et al. [22] were furthest away from our estimates, despite being the only other estimates constructed from GPS tracking data. Their method uses an EV fleet simulator called 'ev-fleet-sim', which is based on the micro-traffic simulator Simulation of Urban MObility (SUMO) and a matching EV kinetic model developed by Kurczveil et al. [33]. Ev-fleet-sim intakes per-minute GPS waypoints, and uses the SUMO routing function to simulate per-second mobility data on an Open Street Maps virtualization of the road infrastructure. This per-second data is run through the kinetic model to estimate energy consumption. A preliminary assessment of their method has shown the inaccuracy of the physical infrastructure virtualization and of the per-second driving simulation as potential reasons for the high consumption rates. Furthermore, in contrast to our simple first-principle kinetic model, theirs is based on the moment of inertia of internal elements, which could also contribute to the difference. A detailed analysis of their method falls beyond the scope of this paper, and is left to future research.

Literature Source	Energy Consumption (kWh/km)	OEM Source	Energy Consumption (kWh/km)
Abraham et al. [22]	0.93	Higer H5C EV [41]	0.36
Cignini et al. [20]	0.70	Dongfeng E-Mini Van [48]	0.27
Collett et al. [24]	0.50	Ruivii Toano [49]	0.26
		Nissan NV Combi [50]	0.21

Table 4: Comparative energy consumption (kWh/km) values seen in the literature and from real-world OEM vehicle specs.

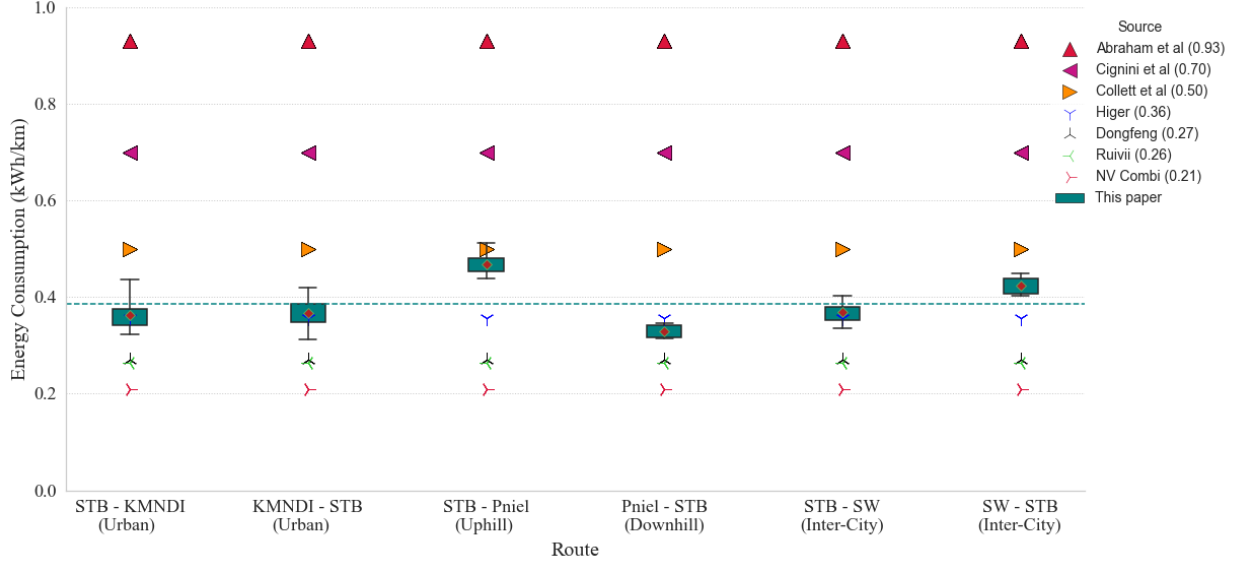


Figure 7: Distributions of energy consumption, compared to state-of-the-art from literature and real world vehicle specs. The dashed teal line represents the mean of the estimates constructed from the per-second data (0.39 kWh/km).

3.2. Implementation of results

The techno-economics of paratransit electrification depend on vehicle energy consumption. Since EV energy demands are known to vary across driving conditions [26], we aim to provide recommendations in multiple conditions. Specifically, we provide recommendations for values to use in urban, inter-city, and hilly (uphill and downhill) conditions. Uphill and downhill are treated separately because if a taxi goes up before a charge and down thereafter, you need two separate numbers for the energy budget as the energy demands are significantly different between the two directions.

3.2.1. Operations planning

Electric minibus taxis in South Africa will need to travel up to 250 km before stopping to recharge [22]. Typically, taxis will operate continuously during the morning and evening rush hour periods from roughly 6AM to 10AM and 5PM to 9PM respectively, and operate at a diminished rate throughout the middle of the day [22, 23]. An electric taxi must be able to sustain operations during the rush hour periods without stopping to charge, lest the driver and owner lose out on profits. Economic loss would discourage uptake of electric taxis and thus the electrification transition, so the highest estimated energy consumption values must be used for planning operations to guarantee continuous operation. However, it is not economic to supply every e-taxi with the largest possible battery pack. An excessively large pack would be unnecessarily expensive and impact payload. A taxi that operates over long distances in a hilly region will not necessarily have the same battery requirements as a taxi that operates for short distances in an urban environment. With this in mind, we provide recommendations in Table 5 that are specific to different conditions. Ranges are calculated as 85% of the battery's physical limit for a given rate of energy consumption, since neither overly deep discharge nor maxing out on charge are good for the health of the battery.

	Urban	Uphill	Downhill	Inter-city
Energy Consumption (kWh/km)	0.44	0.51	0.35	0.45
Range (km) - 50 kWh battery	97	83	122	94
Range (km) - 75 kWh battery	145	125	182	142
Range (km) - 100 kWh battery	193	167	243	189

Table 5: Recommended energy consumption (kWh/km) for calculating range in different driving conditions, based on highest energy consumption observed in each condition. Example ranges (km) using different battery sizes (kWh) are given. Ranges are calculated as 85% of the physical limit that a battery would be able to provide at the given energy consumption.

3.2.2. Grid impact and emissions

In an energy-constrained and coal-dependent context, the interactions between EVs and the electricity grid must be carefully considered when planning the deployment of an EV fleet. Sufficient charging infrastructure and clean energy generation must be available to sustain the fleet, as EV charging can have a substantial impact on the grid [51]. Additionally, policymakers are often interested in the emissions saving of the EV equivalent to an ICE operation, so it is useful for stakeholders to be able to use our estimates to model the greenhouse gas (GhG) emissions impact of transitioning from the status quo an electric fleet.

Since operational (not life-cycle) GhG emissions for EVs depend on their interaction with the electricity grid, the same energy consumption values should be applied for calculating both grid and GhG emissions impact of the fleet. In contrast to operations planning, using an average energy consumption is appropriate for fleet-wide energy demand calculations. Table 6 breaks down the recommended energy consumption values for e-taxi to grid interaction.

	Urban	Uphill	Downhill	Inter-city
Energy Consumption (kWh/km)	0.37	0.47	0.33	0.40

Table 6: Recommended energy consumption (kWh/km) to use for calculating e-taxi impact on the electricity grid in different driving conditions, based on average energy consumption estimated for each route type.

If information on driving conditions is unavailable, we recommend using the overall mean energy consumption of 0.39 kWh/km.

3.3. Effect of mobility characteristics and physical constants on energy consumption

The analysis in this section aims to enable our energy consumption estimates to be generalized for contexts not explicitly captured in our dataset, and for different sets of vehicle physical constant parameters.

For the former, we quantify the effects of net elevation change (m), average speed (m/s), and average absolute acceleration (m/s^2) on energy consumption using Ordinary Least Squares (OLS) regression. The absolute value of acceleration is taken to retrieve the 'total' effect of acceleration and deceleration. For the latter, we compute the sensitivity of our kinetic model to each of the vehicle parameters from Table 1.

Elevation change, speed, and acceleration were chosen as factors to explore because they directly correspond to forces in the kinetic model, but are also comprehensible real-world measurable variables. Respectively, they correspond to slope drag, aerodynamic drag, and vehicle force. Elevation change is accounted for in slope drag via slope angle (Equation 1d), speed enters directly into aerodynamic drag (Equation 1b), and acceleration is derived in vehicle force as change in velocity (Equations 2 and 3)¹.

Despite slope angle being the direct measured factor that enters into the slope drag equation, net elevation change was chosen over average average slope angle because it is an eminently more useful measurement. It is far easier to retrieve net elevation change than average slope angle for routes around the world, and we found that net elevation change approximates slope angle very well. Quantifying the effects of these factors on energy consumption is only useful if the results can be used by stakeholders and other interested parties. Net elevation change and speed limits are easily obtainable features of a route via a quick google search. Including average absolute acceleration in the regression model controls for the effects of 'driver behavior' and other micro-traffic flows on energy consumption that are difficult to ascertain prior to collecting GPS tracking data.

Not only do elevation change, speed, and acceleration correspond to forces experienced by the vehicle in the kinetic model, they are the only measured factors that do so. Consequently, we can be sure that our regression model captures the majority of the variation seen in energy consumption in the data, giving us confidence in the results of the regression. This is borne out by the R-squared seen in our OLS regression of 0.98. R-squared explains the proportion of variation seen in an outcome variable that is captured by the explanatory variables included in a regression model.

¹The last force in the model, rolling resistance (equation 1c), does not have a direct mobility characteristic analog in our model. While slope angle does enter into the rolling resistance equation, this force is primarily a consequence of the physical parameters of mass and rolling resistance coefficient.

3.3.1. Effects of Elevation Change, Speed, and Acceleration

To quantify the effects of net elevation, average speed, and average absolute acceleration on energy consumption, we construct an Ordinary Least Squares (OLS) regression model. OLS regressions estimate model parameters by minimizing the sum of the squared differences between the observed outcome variable (energy consumption in this case), and the outcome predicted by a linear function of the explanatory variables. Our OLS regression results are presented in Table 7.

The coefficients in a regression specify how much the outcome variable changes for a 1 unit increase in each factor:

$$\text{coeff} = \frac{d_{\text{outcome}}}{d_{\text{factor}}}$$

Specifically, the regression in Table 7 shows that an increase of 1 m in net elevation change is predicted to increase energy consumption for a trip by 0.0007 kWh/km, an increase in average speed of 1 km/h is predicted to increase the average energy consumption for a trip by 0.0042 kWh/km, and an increase of 1 m/s² in average acceleration during a trip is predicted to increase energy consumption by 0.4540 kWh/km. These coefficients on net elevation change and average speed are the most useful because they are the two factors easiest to ascertain in the absence of GPS tracking data.

One potentially confusing aspect of these results is the high coefficient on acceleration compared to the other two factors. This is caused by a discrepancy in units. Where net elevation change and average speed vary by tens and hundreds, average acceleration is typically a value between 0 and 1 m/s². To more clearly understand the relative effect of each factor on energy consumption, we construct an standardized OLS regression model with the same factors as in the previous section, as shown in in Table 8. The coefficients in a standardized regression show by how many standard deviations (σ) the outcome variable changes for a 1 σ change in an explanatory variable.

The asterisks next to the regression coefficients indicate the p-value of the coefficient. A p-value less than 0.05 is generally considered statistically significant. We mark $p < 0.001$ by ***, $p < 0.01$ by **, and $p < 0.05$ by *. We find all four factors to be statistically significant to $p < 0.001$. The number in parenthesis below each coefficient is that coefficient's standard deviation. The resultant R-squared of 0.98 demonstrates that the linear model with these four variables captures nearly all of the variation in energy consumption seen in our dataset.

The results from these regressions using the non-standardized model are informative for anyone looking to deploy electric minibuses in other locations with different mobility characteristics. While high sampling frequency GPS data would be ideal for analyzing vehicle energy consumption, it can be difficult or impossible to come by in some circumstances.

	Average Trip Energy Consumption (kWh/km)
Net Elevation Change (m)	0.0007*** (kWh/km per m) [0.0001]
Average Speed (m/s)	0.0042*** (kWh/km per m/s) [0.0006]
Average (absolute) Acceleration (m/s ²)	0.4540*** (kWh/km per m/s ²) [0.0395]
R-squared	0.9780
R-squared Adj.	0.9769

Table 7: OLS Regression model of average speed, net elevation change, and average absolute acceleration on energy consumption. The units on each coefficient are a ratio of the units of the corresponding factor (m, m/s, and m/s³) to the units on energy consumption (kWh/km). The standard deviation of each coefficient is shown in brackets beneath the coefficient. The percentage of the variation in the data captured by the model is shown in the R-squared statistic. The *** indicates 99.9% confidence that the coefficient is statistically significant.

	Average Trip Energy Consumption (σ)
Net Elevation Change (σ)	0.9037*** (σ kWh/km per σ m) [0.0543]
Average Speed (σ)	0.3735*** (σ kWh/km per σ m/s) [0.0542]
Average (absolute) Acceleration (σ)	0.1229** (σ kWh/km per σ m/s ²) [0.0536]

Table 8: Standardized OLS Regression model of net elevation change, average speed, and average absolute acceleration on energy consumption. Each coefficient represents how many standard deviations (σ) energy consumption changes for a 1 standard deviation change in the corresponding factor. The standard deviation of each coefficient is shown in brackets beneath the coefficient. The ** and *** indicate 99% and 99.9% confidence in the statistical significance of the coefficients respectively.

One apparent incongruity between the results in the two regression models is the level of significance of the coefficient on acceleration. It shows *** in the non-standardized model, indicating $p < 0.001$, and ** in the standardized model, indicating $p < 0.01$. This is caused by a discrepancy in units between the two models. Specifically, the coefficient on acceleration in the non-standardized model predicts that energy consumption will change by 0.4540 kWh/km from a 1 m/s² change in average absolute acceleration, whereas the coefficient in the standardized model predicts that energy consumption would change by 0.1229 σ given a 1 σ change in average absolute acceleration.

3.3.2. Effects of model parameters

Next, we assess the sensitivity of the kinetic model to the vehicle physical parameters. The results of the sensitivity analysis are summarized in Table 9. The first column shows the relative sensitivity of the model to each parameter as the percentage change in energy consumption for a 1% change in a given parameter. The second column shows the absolute change in energy consumption in kWh/km for a 1% change in a given parameter. The table shows that the model is most sensitive to powertrain efficiency, followed by the minibus weight, then regenerative braking efficiency and rolling resistance coefficient, then drag coefficient and finally vehicle frontal surface area.

The parameters used for estimations in this paper, listed in Table 1, were carefully chosen from various sources in the literature, but reasonable arguments can be made for different values, and they do vary in the literature [22]. Similar to the results of the OLS regression, the results of the sensitivity analysis are useful to determine the effect of an individual change in each parameter on the energy consumption of taxis. For example, the weight of a taxi could easily change by several hundred kilograms, depending on the weight of passengers and their luggage (aka payload). For example, if the minibus weight parameter was adjusted up by 10% from the value this paper uses (i.e. by 390 kg), to 4.290 kg, then overall mean energy consumption would be expected to increase by 8.4% (i.e. 0.03 kWh/km) to 0.42 kWh/km.

Parameter	Sensitivity ($\frac{\% \text{ change output}}{\% \text{ change input}}$)	Sensitivity ($\frac{\text{absolute change output}}{\% \text{ change input}}$) (kWh/km)
Minibus weight (m_v)	0.84	0.003
Rolling resistance coefficient (c_{rr})	0.48	0.002
Drag coefficient (c_d)	0.15	0.001
Vehicle's front surface area (A)	0.15	0.001
Regenerative braking efficiency (μ_{rg})	-0.50	-0.002
Powertrain efficiency (μ_v)	-1.48	-0.006

Table 9: Sensitivity of kinetic model to physical parameters.

To create Table 9, overall mean energy consumption was simulated with three different input values for each parameter. The center value for each parameter are the values from Table 1. The sensitivities were gathered running the model with each parameter varied twice twice away from the center, while all other parameters were held equal. They varied once above and once below the center value, allowing two equally weighted sensitivities to be calculated for each parameter. The sensitivity reported in Table 9 is the average of the two. The input values are given in Table 10. The values are chosen based on a range of likely operating conditions and values seen in the literature.

Parameter	Values		
Minibus weight (kg)	2900	3900	4900
Rolling resistance coefficient	0.01	0.02	0.03
Drag coefficient	0.24	0.36	0.48
Frontal Area (m ²)	3.50	4.00	4.50
Regenerative braking efficiency(%)	0.50	0.65	0.80
Powertrain efficiency (%)	0.85	0.90	0.95

Table 10: Values used to compute sensitivities of the physical parameters of the kinetic model.

3.4. Evaluation of sampling frequency: Per-second vs per-minute data input

This section explores the energy consumption estimates from per-second data in comparison to energy consumption estimates from an equivalent per-minute dataset.

Throughout the section, the per-second data and associated results are colored in teal and the per-minute equivalent in orange.

The differences between the per-second and per-minute datasets are visualized in Figure 8, which shows the elevation change (m), speed (km/h), and acceleration (m/s²) profiles for an example trip from Pniel - STB. Each plot is accompanied by a chart that quantifies the percentage of that mobility characteristics' signal that is captured in the per-minute sampling frequency. To construct these charts, we perform a Fast Fourier Transformation (FFT) of the per-second data, retrieve the corresponding power spectral density, and compute the percentage of signal captured in sampling frequencies up to $\frac{1}{60}$ Hz (orange bars). The teal bars show the percentage of signal captured by sampling frequencies greater than $\frac{1}{60}$ Hz, up to $\frac{1}{2}$ Hz (the Nyquist frequency for per-second data [30]). These plots show that compared to the per-second data, the per-minute data captures 28.4% of elevation change, 83.4% of speed, and 8.6% of acceleration data. Speed is well approximated in the per-minute data, but the elevation change and acceleration data are much noisier, thus requiring a greater sampling frequency to fully capture. The driving cycle from the per-minute dataset is much smoother, and is unable to account for the micro-mobility movements of the vehicles.

Table 11 characterizes the net elevation change, total absolute elevation change, average speed, and average acceleration profiles by route for the per-minute data in comparison to the per-second data. The table shows that average speed and net elevation change are well characterized in the per-minute data, but crucially, average absolute acceleration and total absolute elevation change are consistently underestimated. Total absolute elevation change was included in this table because, while per-minute data captures overall trends in elevation change, it misses out on the climbs and dips that occur between minutes and contribute to total absolute elevation change. The knock-on effect these oversights have on vehicle energy consumption is explored later in the section.

Together, Figure 8 and Table 11 reinforce the hypothesis that per-minute data does not capture micro-mobility patterns.

Route	Net Elevation Change (m)	Total Elevation Change (absolute) (m)	Average Speed (km/h)	Average Acceleration (absolute) (m/s ²)
STB - KMNDI	17.5 (12.7)	25.2 (92.8)	14.0 (15.9)	0.07 (0.52)
KMNDI - STB	-3.5 (1.3)	169.7 (230.8)	24.4 (26.1)	0.09 (0.57)
STB - SW	-70.5 (-68.1)	423.3 (736.4)	40.3 (42.5)	0.14 (0.50)
SW - STB	67.7 (67.5)	409.6 (755.0)	43.1 (44.2)	0.11 (0.49)
STB - Pniel	126.9 (126.7)	481.2 (797.6)	32.6 (33.2)	0.10 (0.48)
Pniel - STB	-127.2 (-127.2)	457.4 (793.2)	40.6 (40.4)	0.10 (0.52)

Table 11: Characteristics of factors known to influence efficiency in per-minute dataset (orange), compared to the analogous measurements in the per-second dataset (teal) from 3.

The comparison of energy consumption estimates constructed from the per-minute and per-second data is shown in Figure 9. This figure shows that, compared to the per-second data, the per-minute data a) consistently underestimates energy consumption and b) estimates with greater variance. The average overall energy consumption is 31% less than the per-second estimates - 0.27 vs. 0.39 kWh/km - and the average inter-route standard deviation was 0.09 kWh/km, greater than three times higher than the 0.02 kWh/km seen in the per-second estimates. Across all trips, the coefficient of variation for the per-minute estimates was 0.48, more than three times higher than the 0.13 seen in the per-second data.

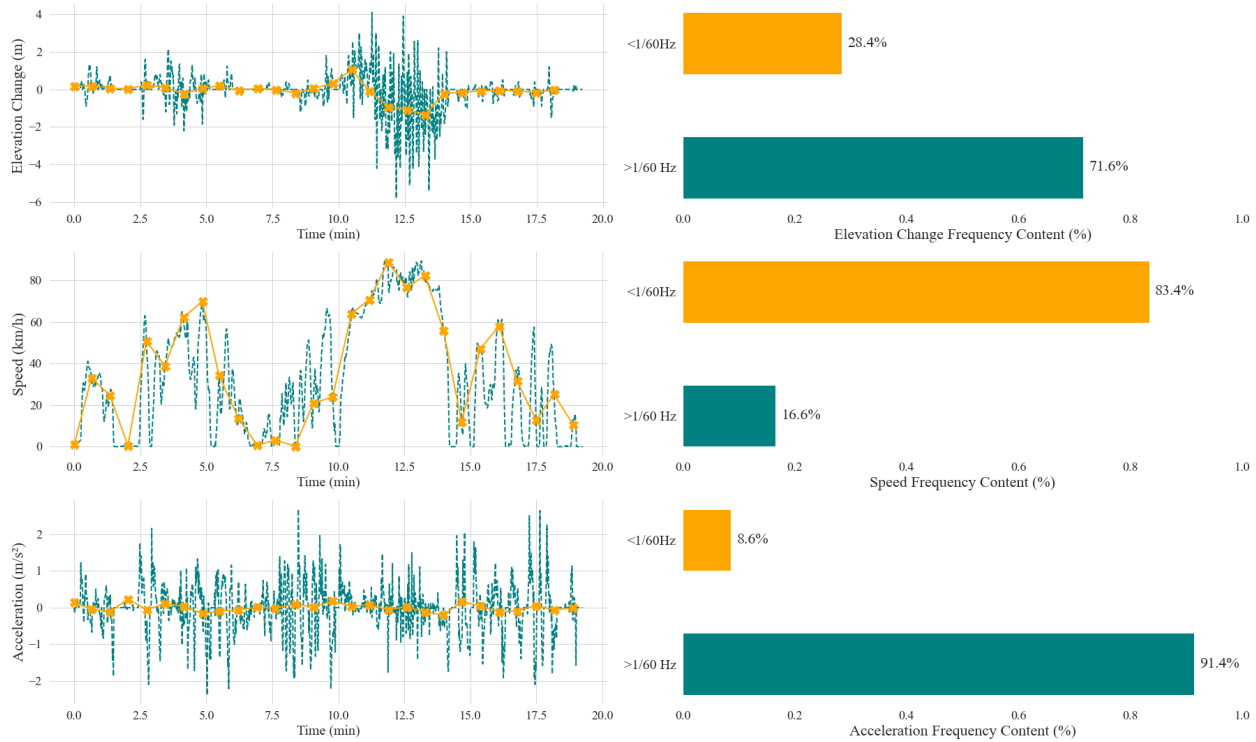


Figure 8: Comparison of the elevation change, speed, and acceleration profiles in the per-second data (dashed teal lines) and per-minute data (solid orange lines) for an example route from Pniel - STB. Each minutely sample on the orange lines is marked with an X. The bar charts show the portion of signal that is captured in the per-minute sampling frequency ($<1/60\text{Hz}$), and the portion of signal that it misses ($>1/60\text{Hz}$) for each factor.

That said, the per-minute data does preserve the relative effect of elevation change, as evidenced by the relatively high energy consumption for the uphill route (STB - Pniel) and low energy consumption for the downhill route (Pniel - STB). This is because per-minute data characterizes net elevation change for the route relatively accurately, despite missing many small dips and climbs that contribute to absolute elevation change and overall energy consumption. The trips with the lowest sample size, the short urban trips to and from Kayamandi (KMNDI), have the greatest variance. Furthermore, the urban route has lower elevation change and speed limits than the hilly or inter-city routes, as well as greater average absolute acceleration. Therefore, following the analysis in Section 3.3, vehicle micro-mobility patterns will have an increased effect on energy consumption in comparison to the other routes. In addition, an analysis of jerk (m/s^3) and number of stops per km along all of the routes also showed that the greatest vehicle jerk and most stop/start driving cycles occurred in the urban context. Therefore, the weakness of the per-minute dataset - its inability to capture micro-mobility patterns - manifests most greatly in the urban environment where environmental characteristics tend to dominate energy consumption less and driver behavior plays a greater role. These findings suggest that per-minute data is least suitable for estimating vehicle energy consumption in urban or residential contexts, which lend themselves to low elevation change, low speed limits, and a larger number of high acceleration/deceleration events (i.e. aggressive driving behavior).

One question remains and that is to quantify where the underestimate in the per-minute data comes from. To do so, we must return to the physics of the kinetic model.

There are six physical forces with distinct effects in the kinetic model, four external, dubbed 'environmental forces', and two forces generated by the vehicle, dubbed 'vehicle forces'. The breakdown is as follows:

- Environmental forces: Propulsive slope drag (downhill), resistive slope drag (uphill), aerodynamic drag, and rolling resistance.
- Vehicle forces: Propulsive (motor to wheels), braking (wheels to motor)

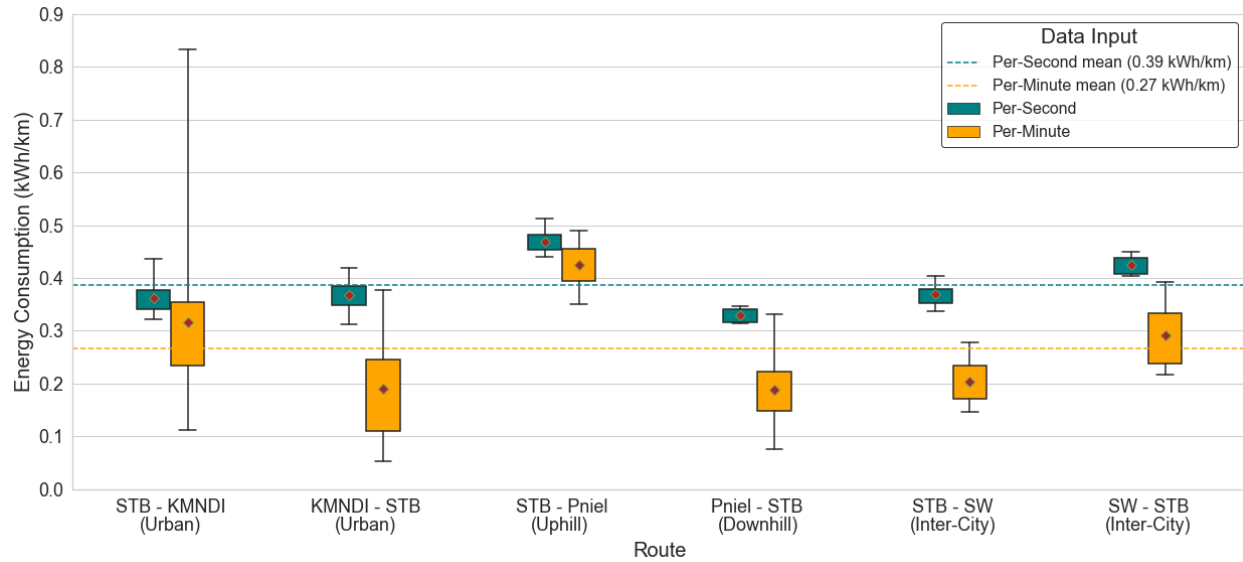


Figure 9: Distribution of energy consumption estimates for each route when the kinetic model is inputted with per-second data versus per-minute data. The dark red diamond in each box represents the mean for that route. The teal and orange dashed lines represent the mean across all trips for the per-second and per-minute inputs respectively. There is one outlier trip at 0.83 kWh/km in STB - KMNDI.

At a fundamental level, the vehicle must generate enough propulsive or braking force to overcome the environmental forces it is experiencing and achieve the driver's desired acceleration or deceleration. Thus, the energy expended by the battery to overcome the environmental forces and achieve the desired acceleration/deceleration can be attributed to environmental forces, and driver behavior. If the per-minute data underestimates the environmental forces and/or the desired acceleration of the driver, then it will underestimate energy consumption.

To quantify where the underestimates in the per-minute model come from, we break down the contribution of each environmental and vehicle force to energy consumption in kWh/km, and perform a FFT to assess how much of this energy is captured by the per-minute sampling frequency. These results are in Figure 10. The top bars represent how much energy in kWh/km are captured in the per-minute data for each force, and the bottom bars represent how much energy the per-minute data misses. The relative size of the bottom bars is not insignificant, thus belying the source of the underestimates from the per-minute dataset input seen in Figure 9.

Table 12 further breaks down the in the energy contribution of each force for each dataset, by route. The largest differences are primarily seen in the two vehicle forces, and the slope drags. This reflects how the per-minute dataset underestimates average absolute acceleration and total absolute elevation change as indicated in Table 11. Net elevation change is well captured, which is reflected in how we can see its effect preserved in Figure 9, in the difference between the uphill and downhill routes. However, missing out on some total absolute elevation change means it underestimates the total contribution of slope drag to energy consumption.

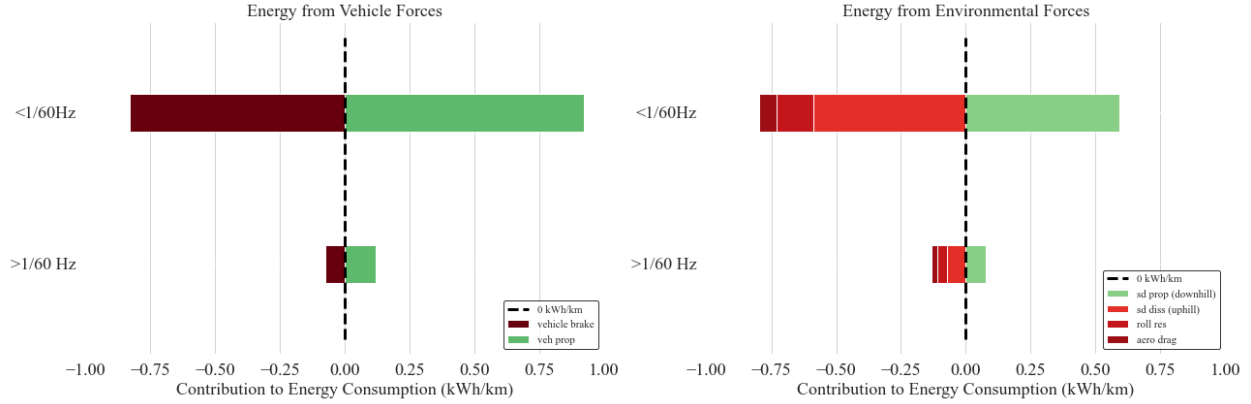


Figure 10: FFT analysis disaggregated by force type. Shows how much energy for each force is captured by sampling frequencies up to once per-minute ($<1/60\text{Hz}$) and greater than once per-minute ($>1/60\text{Hz}$), for all trips. The bottom bar in each graph represents the amount of energy not captured in the per-minute data.

Route	Percentage Difference between Datasets					
	Vehicle Braking	Vehicle Propulsive	Propulsive Slope Drag (downhill)	Dissipative Slope Drag (uphill)	Aerodynamic Drag	Rolling Resistance
KMNDI - STB	-83.5	-61.8	-51.8	-78.5	6.2	12.2
STB - KMNDI	-52.4	-28.7	8.0	9.9	-1.6	10.0
STB - Pniel	-70.1	-25.9	-34.5	-14.6	15.3	12.3
Pniel - STB	-51.7	-46.8	0.1	-43.7	30.0	22.3
STB - SW	-64.8	-51.1	-28.8	-48.8	1.8	0.6
SW - STB	-75.5	-42.0	-37.0	-46.4	6.4	3.0
Mean	-66.3	-42.7	-24.0	-37.0	9.7	10.1

Table 12: Percentage difference between the amount of energy captured in the per-minute and per-second datasets, for each vehicle and environmental force that the vehicle experiences.

This section has shown that per-minute data fails to capture vehicle micro-mobility patterns, thus leading to underestimates of vehicle energy consumption. Per-minute estimates were also found to be high in variance. This supports the initial hypothesis that motivated gathering per-second GPS data: that the per-second data would provide a more accurate picture of paratransit micro-mobility patterns.

4. Conclusions

The aim of this paper is to provide high fidelity energy consumption estimates (kWh/km) for paratransit minibus taxi vehicles, the mainstay of transport in sub-Saharan Africa, in various driving conditions. We estimate paratransit vehicle energy consumption to range from 0.29 - 0.51 kWh/km depending on driving condition. The estimates provided in this paper, based on 1 Hz sampling, are the highest fidelity estimates to date. The lower estimates in this paper compared to previous literature - which provided average estimates from 0.50 - 0.93 kWh/km - imply that the estimated battery capacity requirements and thus cost and grid impact of electric minibus taxis are less than previously suggested, an encouraging result.

Our recommendations can help stakeholders determine e-taxi battery capacity requirements, plan operations, and estimate the electricity demand and emissions impact of deploying e-taxis in varying contexts. Depending on the range requirements and driving condition of its operating region, an e-taxi in South Africa could feasibly require batteries from 50 up to over 100 kWh in size - important for range and cost.

Energy consumption estimates may be needed for dozens or hundreds of different driving conditions around sub-Saharan Africa for planning transitions to electric paratransit. It is practically impossible to capture every combination of these factors seen across the continent in one dataset; however, a benefit of capturing variations in environmental and mobility profiles with high resolution GPS data is that we can quantify the effect of various mobility characteristics on energy consumption. The coefficients in the non-standardized regression model in Section 3.3.1 can be used to extrapolate our results to routes outside of our

dataset that may have different elevation and speed profiles. Similarly, a range of likely operating conditions for e-taxis are possible, and various values are seen in the literature for the parameters on vehicle kinetic models. Accordingly, we quantified the sensitivity of our model to each parameter to allow the effect of adjusting each parameter on our model to be ascertained.

The results show that although per-minute data captures the environmental characteristics of a trip, it misses out on the micro-mobility patterns of a vehicle, leading to underestimates in vehicle energy consumption, and high variance in estimates.

Our results lay the foundation for future work to improve micro-traffic simulators to accurately predict paratransit micro-mobility patterns from origin-destination GPS data of a low sampling frequency. Given the commonality of per-minute GPS data in this field, and the cost and labor requirement of gathering quality per-second data, such improvements would be useful for constructing robust estimates of taxi energy consumption all over sub-Saharan Africa with sparse data.

Acknowledgements

M.J. Booysen and J.H. Giliomee acknowledge financial support from MTN South Africa (Contract S003061) and Eskom (Tertiary Education Support Programme). All authors acknowledge financial support from World Bank project Paratransit Decarbonization in South Africa.

References

- [1] R. Zinkernagel, J. Evans, L. Neij, Applying the sdgs to cities: Business as usual or a new dawn?, *Sustainability* 10 (2018). doi:10.3390/su10093201.
- [2] J. Motavalli, Every Automaker's EV Plans Through 2035 and Beyond, 2021. URL: <https://www.forbes.com/wheels/news/automaker-ev-plans/>.
- [3] Geospatial Commission, Positioning the UK in the fast lane, 2021. URL: <https://www.gov.uk/government/news/the-geospatial-commission-announces-transport-innovation-competition-winners-and-outlines-how-to-position-the-uk-in-the-fast-lane>.
- [4] Sunday Times Driving, Car makers' electric vehicle plans for 2022 and beyond, 2022. URL: <https://www.driving.co.uk/news/new-cars/current-upcoming-pure-electric-car-guide-updated/>.
- [5] N. Pillay, A. Brent, J. Musango, Affordability of battery electric vehicles based on disposable income and the impact on provincial residential electricity requirements in south africa, *Energy* 171 (2019) 1077–1087.
- [6] E. Odhiambo, D. Kipkoech, A. Hegazy, M. Hegazy, M. Manuel, H. Schalekamp, J. Klopp, et al., The potential for minibus electrification in three African cities: Cairo, Nairobi, and Cape Town, Volvo Research and Educational Foundations (2021).
- [7] R. Behrens, D. McCormick, D. Mfinanga, *Paratransit in African cities: Operations, regulation and reform*, Routledge, 2015. doi:10.4324/9781315849515.
- [8] J. Evans, J. O'Brien, B. Ch Ng, Towards a geography of informal transport: Mobility, infrastructure and urban sustainability from the back of a motorbike, *Transactions of the Institute of British Geographers* 43 (2018) 674–688. doi:10.1111/tran.12239.
- [9] D. McCormick, H. Schalekamp, D. Mfinanga, The nature of paratransit operations, in: R. Behrens, D. McCormick, D. Mfinanga (Eds.), *Paratransit in African Cities: Operations, Regulation and Reform*, 1 ed., Routledge, New York, 2016, pp. 59–78.
- [10] KCCA, *Multimodal Urban Transport Master Plan for Greater Kampala Metropolitan Area*, Technical Report, Kampala Capital City Authority (KCCA), Kampala, 2016.
- [11] Transaction Capital, Transaction Capital Results Presentation, 2021. URL: https://thevault.exchange/?get_group_doc=305/1637037219-TCFY21AnalystBooklet.pdf.

- [12] G. Ayetor, I. Mbonigaba, A. K. Sunnu, B. Nyantekyi-Kwakye, Impact of replacing ice bus fleet with electric bus fleet in africa: A lifetime assessment, *Energy* 221 (2021) 119852.
- [13] B. Lin, R. Sai, Towards low carbon economy: Performance of electricity generation and emission reduction potential in africa, *Energy* 251 (2022) 123952.
- [14] D. Ehebrecht, D. Heinrichs, B. Lenz, Motorcycle-taxis in sub-Saharan Africa: Current knowledge, implications for the debate on “informal” transport and research needs, *Journal of Transport Geography* 69 (2018) 242–256. doi:<https://doi.org/10.1016/j.jtrangeo.2018.05.006>.
- [15] J. Brady, M. O’Mahony, Development of a driving cycle to evaluate the energy economy of electric vehicles in urban areas, *Applied Energy* 177 (2016) 165–178. doi:<https://doi.org/10.1016/j.apenergy.2016.05.094>.
- [16] L. Berzi, M. Delogu, M. Pierini, Development of driving cycles for electric vehicles in the context of the city of Florence, *Transportation Research Part D: Transport and Environment* 47 (2016) 299–322. doi:<https://doi.org/10.1016/j.trd.2016.05.010>.
- [17] K. Kivekäs, J. Vepsäläinen, K. Tammi, Stochastic Driving Cycle Synthesis for Analyzing the Energy Consumption of a Battery Electric Bus, *IEEE Access* 6 (2018) 55586–55598. doi:10.1109/ACCESS.2018.2871574.
- [18] R. Smith, S. Shahidinejad, D. Blair, E. Bibeau, Characterization of urban commuter driving profiles to optimize battery size in light-duty plug-in electric vehicles, *Transportation Research Part D: Transport and Environment* 16 (2011) 218–224.
- [19] Q. Wang, H. Huo, K. He, Z. Yao, Q. Zhang, Characterization of vehicle driving patterns and development of driving cycles in Chinese cities, *Transportation Research Part D: Transport and Environment* 13 (2008) 289–297.
- [20] F. Cignini, A. Genovese, F. Ortenzi, A. Alessandrini, L. Berzi, L. Pugi, R. Barbieri, Experimental data comparison of an electric minibus equipped with different energy storage systems, *Batteries* 6 (2020). doi:10.3390/batteries6020026.
- [21] I. Ndibatya, M. J. Booyesen, Characterizing the movement patterns of minibus taxis in Kampala’s paratransit system, *Journal of Transport Geography* 92 (2021) 103001. doi:<https://doi.org/10.1016/j.jtrangeo.2021.103001>.
- [22] C. J. Abraham, A. J. Rix, I. Ndibatya, M. J. Booyesen, Ray of hope for sub-Saharan Africa’s paratransit: Solar charging of urban electric minibus taxis in South Africa, *Energy for Sustainable Development* 64 (2021) 118–127. doi:<https://doi.org/10.1016/j.esd.2021.08.003>.
- [23] M. J. Booyesen, C. J. Abraham, A. J. Rix, I. Ndibatya, Walking on sunshine: Pairing electric vehicles with solar energy for sustainable informal public transport in Uganda, *Energy Research & Social Science* 85 (2022) 102403. doi:<https://doi.org/10.1016/j.erss.2021.102403>.
- [24] K. A. Collett, S. A. Hirmer, H. Dalkmann, C. Crozier, Y. Mulugetta, M. D. McCulloch, Can electric vehicles be good for Sub-Saharan Africa?, *Energy Strategy Reviews* 38 (2021) 100722. doi:10.1016/j.esr.2021.100722.
- [25] A. Zeeman, M. J. Booyesen, Public transport sector driver behaviour : measuring recklessness using speed and acceleration, *Southern African Transport Conference* (2014).
- [26] Y. Al-Wreikat, C. Serrano, J. R. Sodr , Driving behaviour and trip condition effects on the energy consumption of an electric vehicle under real-world driving, *Applied Energy* 297 (2021) 117096. doi:10.1016/j.apenergy.2021.117096.
- [27] M. V. Faria, G. O. Duarte, R. A. Varella, T. L. Farias, P. C. Baptista, Driving for decarbonization: Assessing the energy, environmental, and economic benefits of less aggressive driving in Lisbon, Portugal, *Energy Research & Social Science* 47 (2019) 113–127. doi:<https://doi.org/10.1016/j.erss.2018.09.006>.

- [28] Y. L. Murphey, R. Milton, L. Kiliaris, Driver's style classification using jerk analysis, in: 2009 IEEE Workshop on Computational Intelligence in Vehicles and Vehicular Systems, 2009, pp. 23–28. doi:10.1109/CIVVS.2009.4938719.
- [29] N. E. Eno Akpa, M. Booyesen, M. Sinclair, Fuel savings as an incentive for speed compliance in the informal public transport industry in south africa, in: 2019 IEEE Intelligent Transportation Systems Conference (ITSC), 2019, pp. 492–496. doi:10.1109/ITSC.2019.8917491.
- [30] C. Shannon, Communication in the Presence of Noise, Proceedings of the IRE 37 (1949) 10–21. doi:10.1109/jrproc.1949.232969.
- [31] C. Pan, W. Dai, L. Chen, L. Chen, L. Wang, Driving range estimation for electric vehicles based on driving condition identification and forecast, AIP Advances 7 (2017). doi:https://doi.org/10.1063/1.4993945.
- [32] T. Jonas, C. Hunter, G. Macht, Quantifying the Impact of Traffic on Electric Vehicle Efficiency, World Electric Vehicle Journal 13 (2017). doi:https://doi.org/10.3390/wevj13010015.
- [33] T. Kurczveil, P. Álvarez López, E. Schnieder, Implementation of an Energy Model and a Charging Infrastructure in SUMO, Springer Berlin Heidelberg, 2014, pp. 33–43. doi:10.1007/978-3-662-45079-6_3.
- [34] X. Wu, D. Freese, A. Cabrera, W. A. Kitch, Electric vehicles' energy consumption measurement and estimation, Transportation Research Part D: Transport and Environment 34 (2015) 52–67. doi:https://doi.org/10.1016/j.trd.2014.10.007.
- [35] C. Fiori, K. Ahn, H. A. Rakha, Power-based electric vehicle energy consumption model: Model development and validation, Applied Energy 168 (2016) 257–268. doi:https://doi.org/10.1016/j.apenergy.2016.01.097.
- [36] R. Maia, M. Silva, R. Araújo, U. Nunes, Electric vehicle simulator for energy consumption studies in electric mobility systems, in: 2011 IEEE Forum on Integrated and Sustainable Transportation Systems, 2011, pp. 227–232. doi:10.1109/FISTS.2011.5973655.
- [37] M. Ilyès, A. Fotouhi, N. Ewin, Electric vehicle energy consumption modelling and estimation - A case study, International Journal of Energy Research 45 (2020) 501–520. doi:https://doi.org/10.1002/er.5700.
- [38] I. Sagaama, A. Kchiche, W. Trojet, F. Kamoun, Evaluation of the energy consumption model performance for electric vehicles in sumo, in: 2019 IEEE/ACM 23rd International Symposium on Distributed Simulation and Real Time Applications (DS-RT), 2019, pp. 1–8. doi:10.1109/DS-RT47707.2019.8958704.
- [39] Engineering Toolbox, Rolling Resistance, ND. URL: https://www.engineeringtoolbox.com/rolling-friction-resistance-d_1303.html.
- [40] J. Fridlund, O. Wilen, Parameter Guidelines for Electric Vehicle Route Planning, 2020.
- [41] Higer, Higer H5C EV specifications, ND. URL: <https://en.higer.com/NewEnergy/info.aspx?itemid=6851>.
- [42] Toyota, Toyota HiAce Specifications, ND. URL: <https://toyota.dreamhosters.com/pages/hiace-tmc/spec.php>.
- [43] Toyota, Hiace Ses'fikile Specifications, ND. URL: <https://www.toyota.co.za/specs-compare/hiace-sesfikile?model=CY2>.
- [44] Renault Group, What is the efficiency of an electric motor?, ND. URL: <https://www.renaultgroup.com/en/news-on-air/news/the-energy-efficiency-of-an-electric-car-motor/#:~:text=For%20an%20electric%20vehicle%2C%20energy,not%20a%20very%20large%20amount>.

- [45] Tesla, The Magic of Tesla Roadster Regenerative Braking, ND. URL: <https://www.tesla.com/blog/magic-tesla-roadster-regenerative-braking>.
- [46] USGS, Earth Resources Observation and Science (EROS) Center, ND. URL: <https://www.usgs.gov/centers/eros>.
- [47] Google, Google Earth, ND. URL: <https://earth.google.com/web/@-33.88614835,18.82391936,130.63246104a,12436.34033288d,35y,350.20430081h,0t,0r>.
- [48] T. Dongfeng, Dongfeng Electric 15 Seater Mini Van (RHD), ND. URL: <https://tara-dongfeng.co.uk/listings/dongfeng-ev-15seat-2-2/>.
- [49] Ruivii, Toano 15 Seats Electric Minibus, ND. URL: <https://www.ruviivehicle.com/products/minibus/toano-15-seats-electric-minibus/>.
- [50] Nissan, Nissan e-nv200 combi: Range, charging speed & battery size, ND. URL: <https://www.nissan.co.uk/vehicles/new-vehicles/e-nv200-combi/range-charging.html>.
- [51] K. M. Buresh, M. D. Apperley, M. J. Booysen, Three shades of green: Perspectives on at-work charging of electric vehicles using photovoltaic carports, *Energy for Sustainable Development* 57 (2020) 132–140. doi:10.1016/j.esd.2020.05.007.